

On Feature Decorrelation in Cloth-Changing Person Re-identification

Hongjun Wang, Jiyuan Chen, Renhe Jiang, Xuan Song, and Yinqiang Zheng, *Senior Member, IEEE*.

Abstract—Cloth-changing person re-identification (CC-ReID) poses a significant challenge in computer vision. A prevailing approach is to prompt models to concentrate on causal attributes, like facial features and hairstyles, rather than confounding elements such as clothing appearance. Traditional methods to achieve this involve integrating multi-modality data or employing manually annotated clothing labels, which tend to complicate the model and require extensive human effort. In our study, we demonstrate that simply reducing feature correlations during training can significantly enhance the baseline model’s performance. We theoretically elucidate this effect and introduce a novel regularization technique based on density ratio estimation. This technique aims to minimize feature correlation in the training process of cloth-changing ReID baselines. Our approach is model-independent, offering broad enhancements without needing additional data or labels. We validate our method through comprehensive experiments on prevalent CC-ReID datasets, showing its effectiveness in improving baseline models’ generalization capabilities. **Codes are available at GitHub.**

Index Terms—Long-term person Re-identification, Features Decorrelation.

I. INTRODUCTION

Person re-identification, which aims to match a target person’s image across different camera views, is reported as a crucial task in the field of intelligent surveillance systems [1] and multi-object tracking [2]. Recently, the emergence of Deep Neural Networks (DNNs) has greatly promoted its development, offering promising results in applications. The underlying causal reasoning process of DNNs in the task can be roughly divided into three stages, namely generation, selection and classification, as shown in Fig. 1. In the generation step, the network backbone will generate features from the original image, which normally contain the correlated causal features (e.g., face and gait) and confounding features (e.g., tops and bottoms). Subsequently, the selection process will try to screen out the confounding features to obtain a causal feature representation of the image, which will be used in the following classification to give the final prediction.

In the early researches of ReID [3]–[7], methods are largely studied with cloth-consistent scenarios under the assumption that people do not change their clothes in a short period of time. Generally, these methods can perform well in short-term datasets but will suffer from significant performance

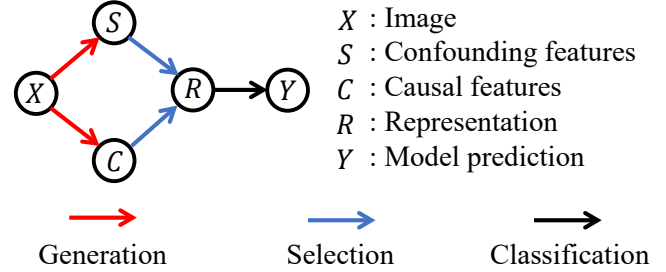


Fig. 1: The causal reasoning diagram for ReID framework.

degradations when testing on a long-term one where people change their clothes frequently. The reason behind such phenomena is very straightforward: unlike human who naturally learns to decouple causality from confounders, DNN tends to exploit the subtle statistical correlations existing in the training distribution for predictions. When trained in a cloth-consistent environment, it creates a strong correlation between the causal and confounding features (e.g., face and cloth appearance) such that the selection process can not effectively discard the latter, and finally resulting in a spurious correlation between the confounding features and person ID. Since the spurious correlation is usually easier to be captured, the model will quickly learn a “shortcut” [8] and ignore all other features (including the true causal features) during inference. However, solely depending on the confounding features is unreliable, since they have large variance across different environments, leading to untrustworthy predictions [9].

To provably avoid the shortcut degeneration problem in ReID, a natural solution is to either incorporate more causal features from other modalities (e.g., contour sketch [10], body shape [11], face/hairstyle [12], [13] and 3D shape [14]) and encourage the model to learn from them, or use hand-crafted clothes labels [15], [16] to force the model pay less attention to the confounding features (mainly the clothes appearance in CC-ReID task). However, obtaining information from multi-modalities requires additional models and training time, and will bring extra bias into the learning of models (i.e., the error in obtaining extra clues from other modality). On the other hand, using additional clothes labels requires much human work, and is not favorable for DNNs which usually requires tremendous amount of data.

Therefore, we are actually motivated back to the root of the problem *i.e.*, feature correlations. Since it is the strong correlation between causal and confounding features that finally leads to the shortcut between confounders and task (e.g., the

Hongjun Wang, Renhe Jiang, and Yinqiang Zheng are with the University of Tokyo, Hongo, Bunkyo City, Tokyo 113-8654. (E-mail: yqzhang@ai.u-tokyo.ac.jp)

Xuan Song is with the School of Artificial Intelligence, Jilin University, Changchun City, Jilin Province.

Jiyuan Chen is with the Department of Computing The Hong Kong Polytechnic University, Hung Hom, Kowloon, Hong Kong.

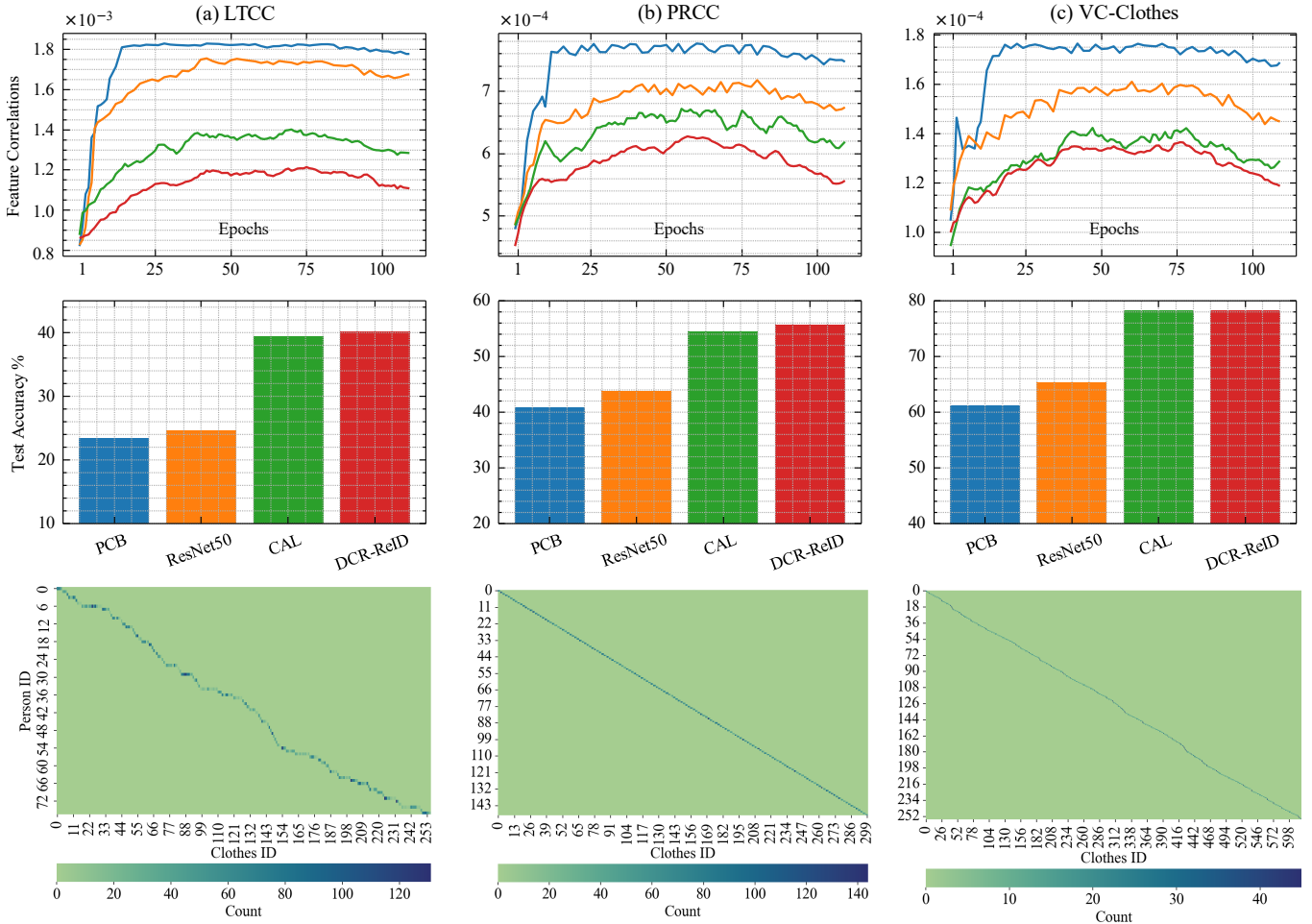


Fig. 2: **This figure shows the intensity of feature correlations generated by the model during training with respect to the model’s final performances.** The upper three figures use the generated features at each epoch to compute the average absolute values of correlation coefficients to represent the correlation between features, whereas the middle figures compute each models’ test accuracy under cloth-changing settings. The corresponding color for each model is the same in both the upper and bottom figures. And, the lower feature illustrate the relation between Clothes ID and person ID in different CC-ReID benchmark.

strongly correlated visual features of red coat and the face of Amy will lead to the shortcut between visual features of red coat with the label ‘Amy’, *what will happen if we simply decorrelate the features in the first place?*

Before going any deeper, let’s first look at some preliminary experiments in Fig. 2. In this figure, we show the intensity of feature correlations generated by the model during training with respect to the final performances. The experiment was run with two cloth-consistent pretrained baselines: PCB [17] and ResNet50 [18], and two cloth-changing baselines: DCR-ReID [16] and CAL [15] on three popular CC-ReID datasets: LTCC [19], PRCC [20] and VC-Clothes [21]. We use the average absolute values of correlation coefficients of generated features to represent the correlation:

$$\rho_{ij} = \frac{\text{cov}(X_i, X_j)}{\sigma_i \sigma_j} = \sum_{I \in \mathcal{D}} \frac{\text{cov}(x_i^I, x_j^I)}{\sigma_i^I \sigma_j^I},$$

and the test accuracy under cloth-changing settings (i.e., only uses cloth-changing samples to calculate accuracy) to indicate

the model performances, respectively. As we can clearly observed from the upper part of the figure, regardless of models and datasets, they all exhibit the same trend during training, that is, a rapid increase of feature correlation in the early epochs, followed by a long and stable period, and finally a mild decrease in feature correlations during the last few epochs. We delve deeper into analyzing the underlying reasons by presenting the statistical results of person ID and clothes ID at the bottom of Fig. 2. It is evident from the data that clothes ID and person ID exhibit a high correlation, indicating that the features of clothes and person are disentangled in hidden state. These observed patterns align very well with previous studies in DNN’s learning principals [22]–[24], which suggest that deep learning models usually experience a fitting phrase and a compression phrase in training, where in the former phrase the model incrementally keeps capturing the correlations that it thinks helpful for fitting the training labels. And in the latter phrase when the training errors become small, the model will start a reduction of its learned correlations,

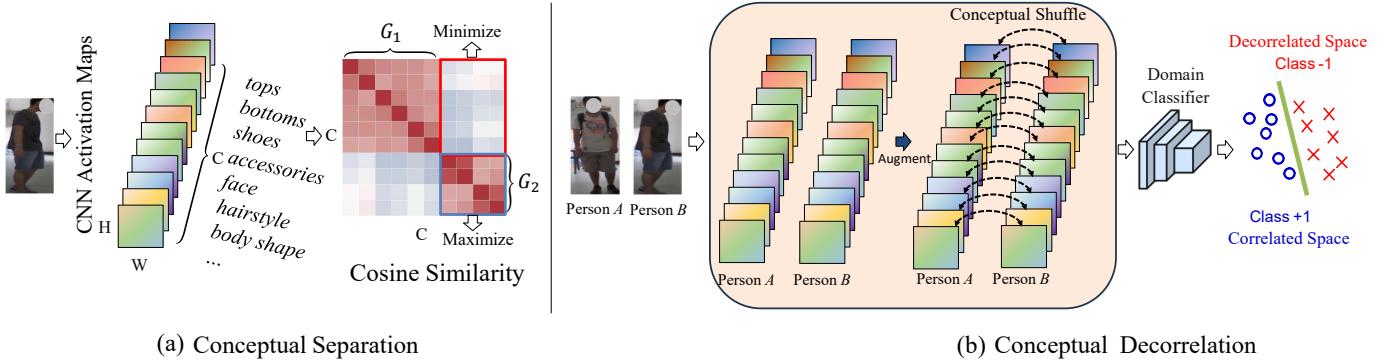


Fig. 3: **Two novel modules are proposed in this work.** We optimize the features cosine distance matrix to generate concept-specific filters. And then, the conceptual shuffle module is used to disentangle the causal features (e.g., face and body shape) and confounding features (e.g., garments and trousers).

which in essence, is to identify and discard the spurious correlations in its best effort to improve generalization. The experiments also demonstrate that within the same dataset, the cloth-changing baselines models, which tend to perform better than others, generally have less feature correlations. Another noteworthy point here is the cloth-changing models also have a higher reduction rate of correlations in the compression phase, which, considering their superior performances, indicates they remove more spurious correlations than the cloth-consistent ones. Moreover, we can observe that there exist some relationships between the modeling difficulty of datasets and the intensity of feature correlations. For example, the same ResNet50 generates features in LTCC that have ten times stronger correlations than those of VC-Clothes. And correspondingly, the test accuracy of ResNet50 in LTCC is much lower than that in VC-Clothes.

Based on the above analysis and observations, a rather simple and intuitive solution to improve model performances in CC-ReID naturally arise, that is to regularize the model for less correlated features. Since we generally don't have ground truth for causal features and confounding features in an image, a softer and conservative way is to decorrelate all the features, so that the model can better select the causal ones without bias. To this end, we propose our *DEnsity RAtio Regularization* (abbreviated as *DEAR* in the following paragraph). *DEAR* computes the density ratio between the model's feature distribution and a "decorrelated" feature distribution which is generated by re-sampling to encourage the model to produce less correlated features. The details of our method are illustrated in Sec. III-A, Sec. III-B and Sec. III-C, while in Sec. III-D we further provide a theoretical explanation why the decorrelation of features could yield better generalization in CC-ReID tasks. Our method is simple and effective, and can be placed over a wide range of current methods to gain extra improvements. Extensive evaluations on public benchmarks has verified effectiveness of *DEAR*, and shows it is a promising direction to explore.

II. RELATED WORK

Many approaches to person Re-identification (ReID) have been proposed, focusing on either clothing-consistent or cloth-

changing scenarios.

A. Clothing Consistent Person ReID.

For clothing-consistent person ReID, early research in person re-identification (re-id) focused on feature extraction [25]–[28] or metric learning [29]–[32], while recent approaches leverage advancements in CNN architectures for end-to-end learning of these aspects [33]–[38]. For example, Sun et al. [17] introduced a part-based convolutional baseline (PCB) module, dividing a feature map into six horizontal blocks for effective ReID. Wang et al. [39] proposed a multibranch network (MGN) for both global and local feature representations, enhancing pedestrian identity discrimination. Gao et al. [40] developed a deep spatial pyramid-based model (DCR) for collaborative feature reconstruction, addressing occlusion and pose changes. Other methods include utilizing human skeleton points or surface texture for guidance. For instance, Song et al. [41] introduced a mask-guided contrastive attention model (MGCAM) with a novel region-level triplet loss, while Miao et al. [42] proposed a pose-guided feature alignment (PGFA) method using key body points to detect occlusions. Gao et al. [43] developed a texture semantic alignment (TSA) approach for partial ReID, addressing occlusion and pose change challenges. However, these models are vulnerable to clothing changes as they heavily rely on the consistency of the appearance of clothes.

B. Clothes Changing Person ReID.

In contrast, cloth-changing person ReID deals with dramatic visual appearance changes over time. Traditional methods are less effective here, prompting the development of specialized datasets like LTCC [11], PRCC [44], Celeb-reID [45], and NKUP [46]. Innovative approaches include Yang et al.'s [44] SPT+ASE module using human contour sketching and spatial polar transformation, and Qian et al.'s [11] shape embedding and clothing-eliminating module (SE+CESD), focusing on body shape. Huang et al. [45] designed the ReIDCaps module using vector neurons to perceive clothing changes. Gao et al. [47] proposed a multigranular visual-semantic embedding

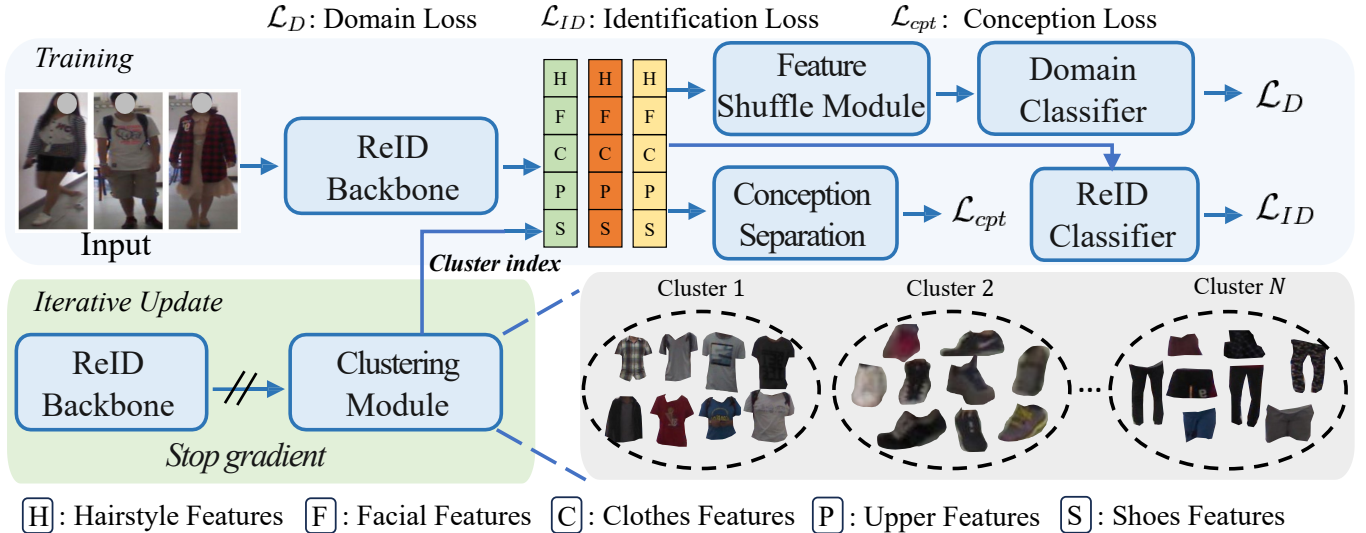


Fig. 4: **The DEAR framework is utilized to achieve feature decorrelation in CC-ReID.** In this figure, distinct colors are used to differentiate between person features. For simplicity and comprehensibility, we assume that only features related to hairstyle, face, upper clothing, lower clothing, and shoes are extracted. First, we apply the K-means algorithm to produce indices for the features generated from the pretrained ResNet50. We periodically update the ReID backbone to ensure accurate labeling of conception indices. Subsequently, DEAR performs a random shuffle of the original person features to produce a decorrelated feature distribution. During each iteration, we begin by optimizing the domain classifier to classify the source of features. Once the domain classifier’s parameters are fixed, we proceed to minimize both \mathcal{L}_{ID} and \mathcal{L}_{cpt} , while maximizing the density ratio loss $\tau(x)$. This dual optimization compels the backbone network to generate features with reduced correlations, thereby enhancing the decorrelation of the feature representations.

algorithm (MVSE), and Hong et al. [48] introduced a fine-grained shape-appearance mutual learning framework. Shu et al. [49] focused on a semantic-guided pixel sampling approach, and Gu et al. [15] introduced a Clothes-based Adversarial Loss (CAL) to mine clothes-irrelevant features. Yang et al. [50] introduce the Auto-Intervention Model (AIM) based on causality to ensure that the learned representation is immune to clothing bias. Cui et al. [16] propose the Component Reconstruction Disentanglement (CRD) module, which separates clothes-irrelevant and clothes-relevant features by reconstructing human component regions. Yang et al. [51] create a win-win scenario by enhancing the identity-preserving information in appearance and structure features while ensuring overall efficiency. Chan et al. [52] utilize a Generative Adversarial Network (GAN) with three encoders, one generator, and three discriminators to separate identity, clothing, and unrelated features. Han et al. [53] examine the influence of clothing on model inference and employ a dual-branch model to mimic causal intervention. As the model is trained, clothing bias is progressively reduced, enabling the Auto-Intervention Model (AIM) to discern more distinctive ID features that are not influenced by clothing bias.

Despite these advancements, existing work mainly try to combine extra data (clothes labels, contour sketch, body shape, 3D shape) to eliminate the clothes related features, which needs additional models and training time. This work proposes a model-agnostic method and provides general improvements without the need of any extra data and label to eliminate the confounding features.

III. METHODOLOGY

While we are seeking to reduce the correlations between features, the first step should be finding a way to effectively measure the intensity of such correlations.

A. Conceptual Separation

In person re-identification, the features of clothes can be biased when the person changes clothes. In this work, as shown in Fig. 1, we aim to eliminate the correlation between the causal features (i.e., the features that are related to the identity of the person) and the confounding features (i.e., the features that are related to the clothes). The first problem we encounter is to identify the concept for each channel in the feature maps. To address this, we first assume that each filter in the convolutional neural network (CNN) consistently represents the same conception. By acquiring the conceptual clustering, we first freeze the model parameters and generate a set of features $H_i = \{h_i^l\}_{I \in \mathcal{D}}$, where I denotes the image sampling from the training dataset \mathcal{D} , and h_i stands for the features map generating by i -th filter. Then, we heuristically use the K-means clustering [54] to divided the set of CNN filters Ω into K groups: $\mathcal{G} = \{G_1, G_2, \dots, G_K\}$ groups, where $G_i \cap G_j = \emptyset$ and $G_1 \cup G_2 \cup \dots \cup G_K = \Omega$. Then, as shown in Fig. 3a, we proposes the penalty term

$$\mathcal{L}_{cpt} = -\frac{1}{K} \sum_{G_k \in \mathcal{G}} \frac{\sum_{i,j \in G_k} s_{i,j}}{\sum_{i,j \in \Omega \setminus G_k} s_{i,j}}, \quad (1)$$

to maximize the inter-group and minimize the intra-group feature map similarity, where $s_{i,j} = \frac{h_i \cdot h_j}{\|h_i\| \|h_j\|}$ denotes the cosine similarity between the i -th and the j -th filters.

B. Conceptual Decorrelation

Before the introduction of density ratio estimation, one may just question why we bother to introduce such concept for feature correlation measurement, since the correlation coefficients seem to perform well in Fig. 2. However, using correlation coefficients requires a huge amount of space and time to save the features and compute the results, which is not widely applicable in today’s training of DNNs. What we need is an on-the-fly measurement that can smoothly integrates with DNN’s training. Fortunately, with a clever use, density ratio estimation [55], [56], an important technique in the unsupervised machine learning toolbox, can help us achieve the goal. Mathematically, the density ratio is defined as follows:

Definition III.1. *The density ratio is defined as the ratio of the density of one distribution p to the density of another distribution q , at a given point in the sample space. Mathematically, the density ratio is expressed as: $\tau(x) = p(x)/q(x)$ where x is a data point in the sample space and $p(x)$ and $q(x)$ are the densities of the two distributions at that point.*

The definition of density ratio looks attractive because in essence it measures how similar the two distributions are. Assuming we have the people’s features from a model’s l^{th} layer, which are represented as $h^l \in n \times d^l$, where n and d^l are the number of people and feature dimensions respectively, if we can further build an uncorrelated data distribution \tilde{h}^l and compute the density ratio between the two, we can then directly measure h^l ’s correlations between its d^l dimensions. Inspired by [49], we construct the uncorrelated data distribution (Fig. 3b) by re-sampling a new distribution \tilde{h}^l from h^l , where $\tilde{h}_{i,j}^l = \text{Random}(h_{k,j}^l)$ and $i \neq k$.

Next, we adopt the probabilistic classification approach [57]–[59], a technique for estimating the density ratio of two classes, to calculate the density ratio. The basic idea is to learn a classifier that separates samples from each class and use the classifier to estimate the density ratio. We start by defining two classes of data with class labels $y = +1$ to $\{h_i\}_{i=1}^N$ and $y = -1$ to $\{\tilde{h}_i\}_{i=1}^M$ with batch size M . The density of each class is represented as $P_h(x) = P(x | y = +1)$ and $P_{\tilde{h}}(x) = P(x | y = -1)$, respectively. Using Bayes’ theorem, the density ratio can be expressed as a ratio of class posterior probabilities $P(y | x)$:

$$\tau(x) = \frac{P_h(x)}{P_{\tilde{h}}(x)} = \frac{P(y = -1) P(y = +1 | x)}{P(y = +1) P(y = -1 | x)}. \quad (2)$$

The prior probability of each class, $P(y = -1)$ and $P(y = +1)$, can be approximated as the ratio of the number of samples in each class. The class posterior probability $P(y | x)$ can be estimated using a probabilistic classifier, such as Multilayer perception (MLP). In a probabilistic classifier, a function is trained to predict the class label for a given input sample, and the class posterior probability can be obtained as

the output of the function. The density ratio estimator can then be calculated as the ratio of class posterior probabilities. Until now, we can effectively compute the features’ correlations during training. In the next section, we will formally introduce how *DEAR* works to decorrelate the features.

C. Training Procedure

The overall framework of *DEAR* is depicted in Fig. 4. Our training procedure can be divided into two steps:

- **Stage I:** we apply the K-means algorithm to produce indices for the features generated from the pretrained ResNet50, periodically updating the ReID backbone in several epoch for accurate labeling. Subsequently, *DEAR* performs a random shuffle of the person features to create a decorrelated distribution.
- **Stage II:** After stage I, we start by optimizing the domain classifier to identify the source of features. Once the domain classifier’s parameters are fixed, we minimize both $\mathcal{L}_{\mathcal{ID}}$ and \mathcal{L}_{cpt} , while maximizing the density ratio loss $\tau(x)$. This dual optimization encourages the backbone network to produce features with reduced correlations, enhancing the overall decorrelation of the feature representations.

We thereafter formally give the definition of

Training Identity Classifier. Let x_i be a data sample of person re-id, and y_i^{ID} be its label. We further have C_φ as the person ID classifier with parameter φ and g_θ is the backbone parameterized by θ . Fundamentally, we use the cross entropy loss \mathcal{L}_{PID} as:

$$\min_{\varphi} \mathcal{L}_{\mathcal{ID}} (C_\varphi (g_\theta (x)), y_i^{ID}), \quad (3)$$

Training Domain Classifier. To combine density estimation in clothes changing person reid, this paper adds a new domain classifier to the existing re-id model. The domain classifier \mathcal{D} has parameters ϕ , and its purpose is to predict the domain class of an input feature (i.e., whether it belongs to the original class or the uncorrelated class). During training, the domain classifier is optimized by minimizing the domain classification loss, which is calculated as a cross-entropy loss $\mathcal{L}_{\mathcal{D}}$ between the predicted domain class and the actual domain label:

$$\min_{\phi} \mathcal{L}_{\mathcal{D}} (\mathcal{D}_\phi (g_\theta (x)), y), \quad x \in \{h_i\}_{i=1}^N \cup \{\tilde{h}_i\}_{i=1}^M \quad (4)$$

In each iteration of training, the model parameters are updated in two steps: first, the domain classifier parameters ϕ are optimized by minimizing the clothes classification loss (Eq. (4)); and second, we fix parameter ϕ and the backbone parameters θ of the re-id model are updated to minimize the re-id loss.

D. Theoretical Analysis

We now theoretically prove that the decorrelation operation could help us to eliminate the confounding features.

Notations. The d -dimensional features are represented by $X = (X_1, X_2, \dots, X_d)^T \in \mathbb{R}^d$, and the outcome is denoted by $Y \in \mathbb{R}$, based on a joint training distribution $P^{\text{tr}}(X, Y)$. The test distribution, which is unknown, is denoted by P^{te} , while \tilde{P} refers to a specific target distribution that satisfies

$\text{Cov}_{\tilde{P}}[XX] = 0$. $X_i \in \text{Causal}(Y)$ denotes the X_i is the causal features contributing to Y , such as human face, or body shape. In this paper, the objective function used is the least squares to represent the feature selection procedure since it has a closed-form solution.

$$\hat{\beta} = \arg \min_{\beta} \mathbb{E} \left[(\beta^T X - Y)^2 \right] = \text{Var}(X_i)^{-1} \text{Cov}[X_i Y].$$

Theorem III.1. *if $X_i \notin \text{Causal}(Y)$ and $X_i \sim \tilde{P}$, then the solution β of weighted least squares satisfies $\beta(X_i) = 0$. Here, $\beta(X_i)$ refers to the coefficient on X_i .*

Proof. Let X_{-i} be the set of variables in X excluding X_i , and let \mathcal{X}_{-i} be the support of X_{-i} . Assuming $X_i \notin \text{Causal}(Y)$, there exists a function $f : \mathcal{X}_{-i} \rightarrow \mathcal{Y}$ such that $\mathbb{E}_{P^{\text{tr}}(X,Y)}[Y | X] = f(X_{-i})$. We also assume that $\mathbb{E}_{\tilde{P}(X,Y)}[Y | X] = \mathbb{E}_{P^{\text{tr}}(X,Y)}[Y | X] = f(X_{-i})$. As a result, the covariance between X_i and Y under \tilde{P} is given by

$$\begin{aligned} \text{Cov}_{\tilde{P}}[X_i Y] &= \mathbb{E}_{\tilde{P}(X_i, Y)}[X_i Y] - \mathbb{E}_{\tilde{P}(X_i)}[X_i] \mathbb{E}_{\tilde{P}(Y)}[Y] \\ &= \mathbb{E}_{\tilde{P}(X)}[X_i f(X_{-i})] - \mathbb{E}_{\tilde{P}(X_i)}[X_i] \mathbb{E}_{\tilde{P}(X_{-i})}[f(X_{-i})] \\ &= 0. \end{aligned}$$

The last equation follows from the fact that X_i and X_{-i} are independent in the distribution \tilde{P} . Thus, we can write

$$\beta(X_i) = \text{Var}_{\tilde{P}}(X_i)^{-1} \text{Cov}_{\tilde{P}}[X_i Y] = 0$$

Theorem III.2. *if $X_i \in \text{Causal}(Y)$ and $X_i \sim \tilde{P}$, then there exists a constant $\alpha \neq 0$, such that the solution β satisfies $\beta(X_i) = \alpha$. Here, $\beta(X_i)$ refers to the coefficient on X_i .*

Proof. We define X_{-i} to be the set of variables in X excluding X_i , and P_{-i}^{tr} to be the marginal distribution of P^{tr} on X_{-i} . Since X_i is a causal variable of Y , we know that $\mathbb{E}_{P^{\text{tr}}(X,Y)}[Y | X]$ depends on X_i . This implies that there exists a probability density function \tilde{P}_{-i} with the same support as P_{-i}^{tr} such that X_{-i} are mutually independent under \tilde{P}_{-i} , i.e., \tilde{P}_{-i} factorizes over X_{-i} . Furthermore, there exists a probability density function \tilde{P}_i with the same support as P_i^{tr} such that $\mathbb{E}_{P^{\text{tr}}(X,Y)}[Y | X]$ is linearly correlated with X_i under \tilde{P}_i . This means that $\mathbb{E}_{\tilde{P}(X,Y)}[Y | X]$ is also linearly correlated with X_i . Since $\mathbb{E}_{P^{\text{tr}}(X,Y)}[Y | X]$ depends on X_i , we know that $\text{Var}_{P^{\text{tr}}}(X_i) > 0$. Therefore, $\text{Var}_{\tilde{P}}(X_i) > 0$. Letting $Z = \mathbb{E}_{P^{\text{tr}}(X,Y)}[Y | X]$, the coefficient on X_i is the covariance between X_i and Z divided by the variance of X_i , which is given by

$$\begin{aligned} \beta(X_i) &= \frac{1}{\text{Var}_{\tilde{P}_i}(X_i)} \left(\mathbb{E}_{\tilde{P}(X_i, Y)}[X_i Y] - \mathbb{E}_{\tilde{P}(X_i)}[X_i] \mathbb{E}_{\tilde{P}(Y)}[Y] \right) \\ &\sim \mathbb{E}_{\tilde{P}_i(X_i)}[X_i Z] - \mathbb{E}_{\tilde{P}_i(X_i)}[X_i] \mathbb{E}_{\tilde{P}_i(X_i)}[Z] \neq 0 \end{aligned}$$

IV. EXPERIMENTS

In this study, a new framework is proposed for clothing person ReID, and its performance is evaluated on

three publicly available datasets: PRCC [20], LTCC [19], VC-Clothes [21]. The proposed method is evaluated using two common metrics, namely top-1 accuracy, and mAP, and three different test settings are defined to assess its capabilities. These settings include the general setting, which utilizes both clothes-consistent and clothes-changing samples to calculate accuracy; the clothes-changing setting (CC), which only uses clothes-changing samples; and the same-clothes setting (SC), which only uses clothes-consistent samples. For LTCC dataset, the re-identification accuracy is reported for both the general and clothes-changing settings. Regarding PRCC, the re-identification accuracy is reported for both the same-clothes and clothes-changing settings, following the methodology outlined in [20]. In terms of VC-Clothes, we tested it on two groups of cameras, (1) camera 2&3 measured the accuracy for the same clothes scenario (SC), (2) camera 3&4 measured the accuracy for the clothes-changing scenario (CC).

A. Comparison with State-of-the-art Methods

In our study, we benchmarked the proposed method against various leading ReID models on LTCC, PRCC datasets, as shown in Tab. I, including both standard ReID models like BoT [64], PCB [17], MGN [39], SCPNet [66], ISGAN [67], AIM [50], CAL [15], and OSNet [4], and those tailored for clothes-changing scenarios, such as LTCC [11], CASE [63], FSAM [61], CCFA [53], and 3DSL [62]. Chan et al. [52] implemented all models using available codes, with the exception of a few ([10]–[12], [63]) which were replicated based on their descriptions in the papers. It should be noted that the clothes-changing re-id methods use information from different modalities to mitigate the interference of clothes, with 3DSL and FSAM integrating at least three modalities. However, the computational cost of these two methods is at least four times higher than that of DEAR. In addition, RCSANet utilizes additional clothes-consistent re-id data to enhance performance in the same-clothes setting. Nevertheless, without using additional data and only using RGB images in the backbone of ResNet50, the proposed DEAR consistently outperforms all of these methods on both datasets. This comparison highlights the effectiveness of DEAR. Additionally, we further evaluated DEAR on another cloth-consistent method (TransReID [69] and OSNet [4]) across varied benchmarks except for ResNet50.

B. Implementation Details

For image-based datasets (LTCC, PRCC, and VC-Clothes), the output feature map is subjected to global average pooling and global max pooling, as outlined in [71]. The resulting features are concatenated, normalized through BatchNorm [72], and the input images are resized to 384×192 , as per [19]. Random horizontal flipping, cropping, and erasing [73] techniques are applied for data augmentation. Training is carried out for 150 epochs, with a batch size of 64, which contains 8 persons and 8 images per person, utilizing Adam [74]. The learning rate is set at $3.5e^{-4}$, with a 10-fold decrease every 20 epochs.

TABLE I: **Comparison with state-of-the-art methods on LTCC, and PRCC.** The results indicated by an underline were copied from the original papers. A backslash indicates that a result is not available. The Extra data indicates, such as, contour sketches, silhouettes, human poses, and 3D shape information.

Methods	Cloth labels	Extra data	LTCC						PRCC					
			General			CC			Same Clothes			CC		
			mAP	Rank1	Rank5	mAP	Rank1	Rank5	mAP	Rank1	Rank5	mAP	Rank1	Rank5
LTCC [19]		✓	<u>34.31</u>	<u>71.39</u>	\	<u>12.40</u>	26.15	\	89.37	96.08	98.24	28.89	30.45	38.98
3APF [12]		✓	21.37	54.41	70.23	9.72	22.43	38.76	95.02	98.04	99.69	41.63	43.95	54.58
ReIDCaps [60]			15.81	43.03	58.61	6.20	12.82	23.71	96.62	99.54	99.61	44.81	48.00	54.61
FSAM [61]		✓	<u>35.4</u>	<u>73.2</u>	\	<u>16.2</u>	<u>38.5</u>	\	—	98.8	100.0	—	54.5	86.4
3DSL [62]	✓	✓	\	\	\	<u>14.8</u>	<u>31.2</u>	\	—	\	\	—	51.3	86.5
CASE [63]	✓		21.10	52.70	70.59	9.86	22.96	38.52	96.18	98.89	99.41	36.68	42.90	56.34
FD-GAN [52]	✓		36.89	73.43	80.12	15.36	32.91	46.68	99.69	99.97	100.00	58.57	58.34	63.82
CAL [15]	✓		40.8	74.2	\	18.4	40.9	\	99.8	100	\	55.8	55.2	\
AIM [50]	✓		41.1	76.3	\	19.1	40.6	\	99.9	100	\	58.3	57.9	\
CCFA [53]	✓		42.5	75.8	\	22.1	45.3	\	98.7	99.6	\	58.4	61.2	\
DCR-ReID [16]	✓	✓	42.3	76.1	\	20.4	41.1	\	99.7	100	\	57.4	57.2	\
BoT [64]			27.80	64.33	76.91	10.70	28.12	42.12	98.41	99.30	99.82	45.31	44.92	52.51
PCB [17]			30.39	64.50	76.27	11.24	21.27	38.78	97.01	99.02	99.90	37.56	36.49	43.75
Part-aligned [65]			21.33	53.18	69.61	9.58	21.41	38.50	95.63	98.70	99.82	39.33	42.24	51.51
MGN [39]			33.85	66.32	74.95	13.69	27.30	41.34	98.77	99.92	99.97	53.12	54.12	61.71
SCPNet [66]			18.02	48.07	67.34	7.38	15.82	31.63	93.09	97.68	99.10	23.48	22.92	35.39
ISGAN [67]			33.76	68.56	77.69	<u>13.03</u>	29.08	42.86	99.65	99.90	100.00	55.97	54.09	59.74
DGNet [68]			32.18	64.71	78.30	10.80	21.70	34.69	97.42	99.15	99.85	48.17	49.08	63.53
ResNet50 [18]			29.41	65.57	73.80	11.05	28.16	42.13	98.44	97.90	99.81	43.36	45.67	52.32
+DEAR w.o. Decor			34.75	71.05	79.38	15.44	35.22	47.26	99.47	99.81	100.00	51.11	49.15	56.48
+DEAR w.o. Adv			31.88	68.89	77.78	14.00	33.48	47.40	99.13	99.88	100.00	50.66	48.88	55.46
+DEAR			38.18	73.72	80.17	17.55	42.18	54.10	99.88	99.93	100.00	57.57	58.06	63.82
OSNet [4]			32.14	67.86	75.88	10.76	23.92	40.17	97.20	99.35	99.54	30.52	30.06	37.12
+DEAR w.o. Decor			36.21	72.45	80.12	14.33	36.78	50.89	99.55	99.82	99.93	45.76	42.34	48.42
+DEAR w.o. Adv			33.67	70.21	78.45	12.89	34.90	49.21	99.37	99.74	99.92	43.21	40.78	47.09
+DEAR			38.75	74.77	81.88	17.68	44.33	55.83	99.89	99.91	100.00	52.81	53.05	59.88
TransReID [69]			33.08	63.74	74.00	15.17	26.88	43.19	99.89	99.99	100.00	43.08	48.96	51.22
+DEAR w.o. Decor			35.76	72.81	80.52	13.97	36.56	50.38	99.48	99.66	99.85	50.34	52.08	59.69
+DEAR w.o. Adv			33.06	69.72	78.18	12.87	34.89	49.61	99.32	99.77	99.94	50.03	50.60	57.24
+DEAR			39.25	75.22	81.38	17.41	44.02	55.78	99.81	99.83	99.94	58.99	59.22	64.62

TABLE II: **Comparison with state-of-the-arts on VC-Clothes.**

method	General (all cams)		SC (cam2&cam3)		CC (cam3&cam4)	
	top-1	mAP	top-1	mAP	top-1	mAP
MDLA [70]	88.9	76.8	94.3	93.9	59.2	60.8
PCB [17]	87.7	74.6	94.7	94.3	62.0	62.2
Part-aligned [65]	90.5	79.7	93.9	93.4	69.4	67.3
FSAM [61]	-	-	94.7	94.8	78.6	78.9
3DSL [62]	-	-	-	-	79.9	81.2
CAL [15]	92.9	87.2	95.1	95.3	81.4	81.7
ResNet50	88.3	79.2	94.1	94.3	67.3	67.9
+DEAR	94.5	89.4	95.4	95.4	90.1	83.7

C. Attention Map

To determine the cues learned by the model, heat maps were visualized using different clothes-consistent baselines as shown in Fig. 6. Class activation mapping (CAM) [75] was used to generate these heat maps, with pixel brightness indicating the level of attention paid by the model. The second and third columns of this figure show how the model’s attention to different image features changes with and without DEAR in ResNet50. Our analysis showed that the baseline models primarily focused on clothing, with little attention paid to the head due to the low proportion of head pixels. This led to poor performance in cloth-changing settings. In

contrast, our method prioritizes the head and shoes, with a focus on facial features as demonstrated in Fig. 6. Surprisingly, our regularization appears to be a feature selection procedure that highlights the causal features that hair and shoes serve as important cues for our method from a biased feature set, as evidenced by a comparison of the attention maps.

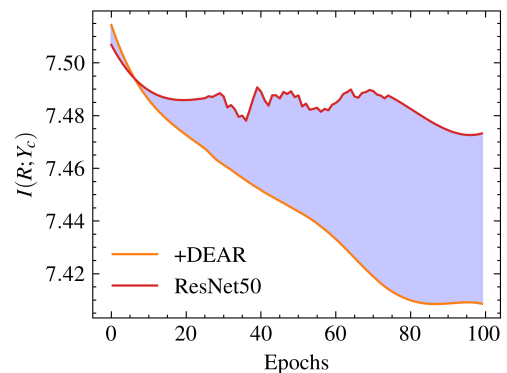


Fig. 5: Mutual information between representation and clothes in ResNet50 performing on LTCC datasets.

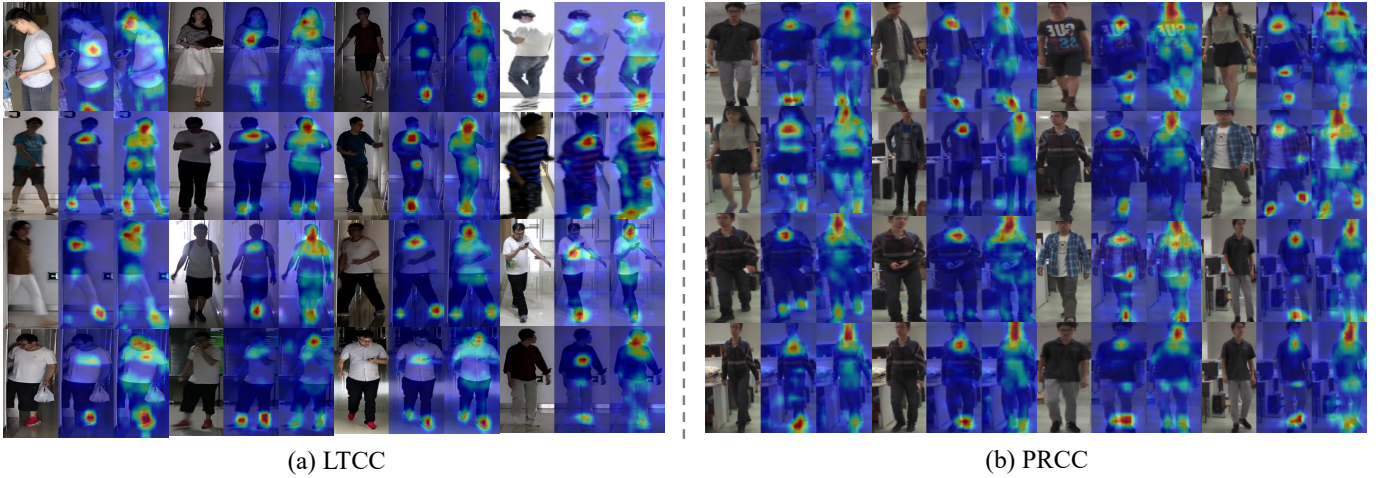


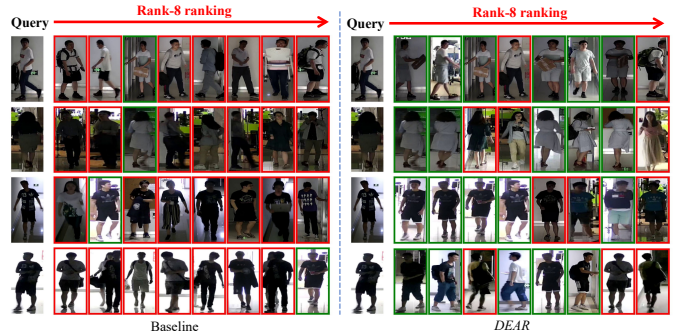
Fig. 6: The comparison between the feature maps with and without our strategy in ResNet50. The first row shows the original image frames from the PRCC dataset. The second and third rows depict the feature maps of the baseline method and *DEAR*, respectively.

TABLE III: Comparison with state-of-the-art methods on LaST and DeepChange.

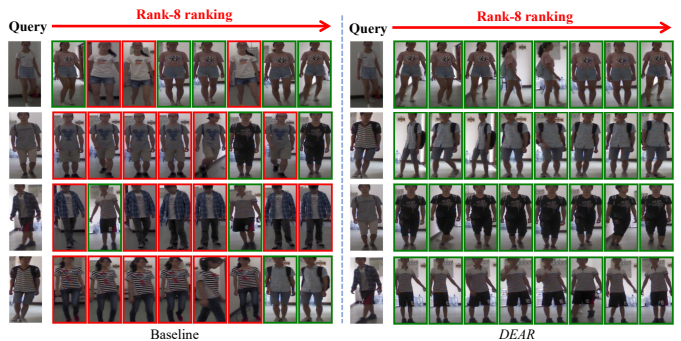
method	LaST		DeepChange	
	top-1	mAP	top-1	mAP
OSNet [76]	63.8	20.9	39.7	10.3
ReIDCaps [60]	-	-	39.5	11.3
BoT [77]	68.3	25.3	47.5	13.0
mAPLoss [78]	69.9	27.6	-	-
CAL [15]	73.7	28.8	54.0	19.0
ResNet50	69.4	25.6	50.6	15.9
+ <i>DEAR</i>	72.1	27.9	53.1	18.4

V. LAYER SELECTION FOR APPLYING *DEAR*

Our investigation focuses on determining the optimal locations in a network to apply *DEAR*. In Table IV, we explored three possible variants for substituting *DEAR* for these bottlenecks. These are (1) ResBlock-D2, where *DEAR* inserts the $\{2n, n = 1, 2, \dots, 8\}$ -th bottlenecks, (2) ResBlock-D4, where *DEAR* inserts the $\{4n, n = 1, 2, \dots, 8\}$ -th bottlenecks, and (3) ResBlock-D8, where *DEAR* inserts the $\{8n, n = 1, 2, \dots, 8\}$ -th bottlenecks. In Table IV, we investigated other possible variants for substituting *DEAR* for these bottlenecks. These are ResBlock-P1, ResBlock-P2, ResBlock-P3, ResBlock-P4, which plug *DEAR* in the layer-1, layer-2, layer-4, layer-4, respectively. We also examined the performance of *DEAR* with L_1 regularization. Our findings, illustrated in Table IV, indicate that a majority of *DEAR* models outperform the baseline, with networks that incorporate full *DEAR* performing worse. Furthermore, we observed that 'ResBlock-D4' and 'ResBlock-P1' achieved a higher test accuracy of 34.20% and 33.30%, respectively. We attribute this to the model adjustment on the correlated output provided by *DEAR*, which improves the model's representation ability. Additionally, *DEAR* with L_1 had a test accuracy of 33.60%, consistently higher than the baseline and *DEAR* only. We conjecture that L_1 further increases the information compression ability.



(a) LTCC



(b) PRCC

Fig. 7: A comparative analysis of Rank-8 retrieval results using both the baseline method and *DEAR* approach in LTCC and PRCC dataset.

A. Evaluation on VC-Clothes

To showcase the superiority of *DEAR*, we also evaluate it using the VC-Clothes dataset, a synthetic virtual dataset from GTA5 as documented in Real et al. [21] and Hong et al. [61], focus on a subset of the dataset from cameras 2 and 3, known as the same-clothes (SC) setting. They also consider another subset from cameras 3 and 4, termed the clothes-

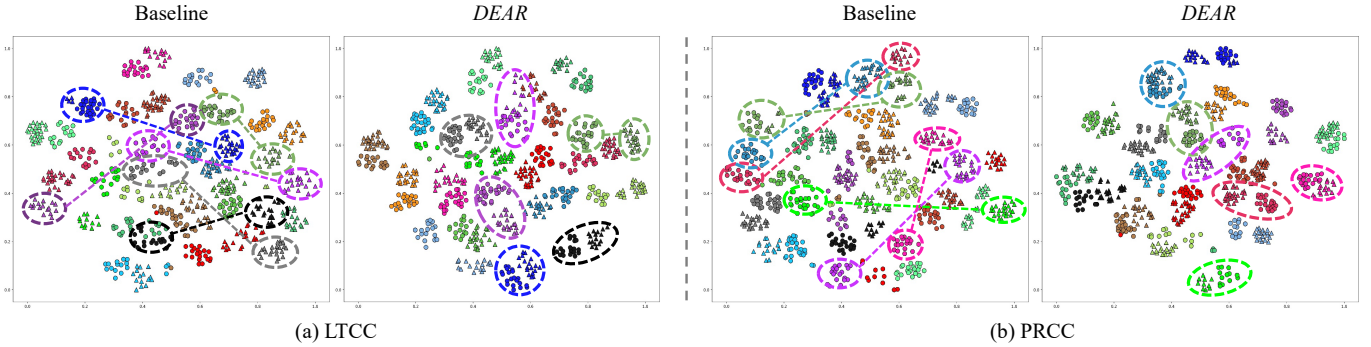


Fig. 8: Each distinct color in the visualization corresponds to a different individual. Images represented by dots and crosses are from different clothing status.

changing (CC) setting. For consistency and fair comparison, our study adopts these standard evaluation settings. To validate the effectiveness of *DEAR*, we compare it against two single-modality-based re-identification (re-id) methods: MDLA [70] and PCB [17], one clothes label-based method CAL [15], and three multi-modality-based re-id methods: Part-aligned [65], FSAM [61], and 3DSL [62], using the VC-Clothes dataset. The comparative results are detailed in Table II. Significantly, *DEAR*, consistently surpasses both the baseline and all the aforementioned state-of-the-art methods in every evaluated metric. This includes overall performance, performance in the same-clothes setting, and the clothes-changing setting, underscoring its effectiveness in various scenarios.

B. Evaluation on Large-scale Datasets

LaST [78] and DeepChange [79] represent two significant long-term person re-identification (re-id) datasets. LaST, a large-scale dataset, comprises over 228,000 meticulously annotated pedestrian images sourced from various movies. This dataset is instrumental for exploring scenarios involving pedestrians with extensive activity ranges and prolonged time spans. On the other hand, DeepChange encompasses a collection of 178,000 bounding boxes from 1,100 distinct person identities, amassed over a year. For a balanced evaluation as per [15], we standardized the batch size to 64, with each batch encompassing 16 individuals and 4 images per individual. The performance metrics of *DEAR* and other methods including OSNet [76], ReIDCaps [60], BoT [77], mAPLoss [78], and CAL [15], are presented in a generalized setting. Specifically, for DeepChange, true matches were permitted from the same camera but distinct tracklets in line with the dataset’s guidelines [79]. As illustrated in Table III, *DEAR* showcases superior performance over both baseline and contemporary state-of-the-art methods in the context of LaST and DeepChange datasets. Particularly noteworthy is the effectiveness of *DEAR*, especially in comparison to CAL, which employs the date of collection as an alternative to clothing labels.

C. Evaluating the Clothes Relevant Features

Drawing inspiration from Tishby et al. (2015) [24], we adopt the mutual information metric $I(R; Y_c) = H(R) - H(R | Y_c)$ to evaluate the interdependence between the representation and

clothing labels. This measure assesses how much one random variable informs about the other and is characterized by its symmetric nature, meaning it remains unchanged regardless of the order of the variables. Our results, particularly with ResNet50’s performance on the LTCC dataset, are graphically depicted in Fig. 5. Consistent with the observations in [24], the network initially focuses on accurately representing the input data, thereby minimizing generalization error. It then transitions to a phase of compressing the input representation, selectively disregarding non-essential details. Consequently, ResNet50 undergoes a dual-stage process aimed at diminishing clothes-relevant features. However, as illustrated in Fig. 6, this approach proves insufficient. In contrast, the implementation of ResNet50 with the *DEAR* plug-in demonstrates a consistent elimination of clothing information throughout the entire process. This distinction underscores the efficacy of *DEAR* in enhancing the model’s ability to focus on more relevant features beyond mere clothing attributes.

D. Retrieval Result Visualization

The effectiveness of the *DEAR* model is demonstrated through retrieval results on the LTCC and PRCC dataset, as presented in Fig. 7. In each retrieval scenario, correctly matched images are indicated with green boxes, while incorrect matches are marked with red ones. Overall, *DEAR* significantly enhances the accuracy of retrieval, yielding more correct matches to the clothes changing scenario in top-ranked positions compared to the baseline. This demonstrates *DEAR*’s capability in improving retrieval accuracy by feature decorrelation.

E. Feature Visualization

We also present a visualization of feature distributions using t-SNE [80] in a 2D feature space, as shown in Fig. 8. In this visualization, distinct colors represent different individuals. Each person maintains the same color throughout the various images. The dot symbol signifies images captured while the individuals were wearing specific clothing. Conversely, the cross symbol denotes images captured when they were not wearing that clothing. This visualization reveals that methods *DEAR* effectively distinguish and cluster feature embeddings of the same individual with different clothing status, demonstrating

TABLE IV: Impact of *DEAR* Module Positioning on ResNet-50 Performance on Cloth-changing.

Methods	LTCC		PRCC	
	R-1	mAP	R-1	mAP
ResBlock P_0	29.8	12.7	52.1	51.3
ResBlock P_1	34.2	13.5	54.7	55.1
ResBlock P_2	38.6	16.8	55.3	53.2
ResBlock P_3	40.1	17.5	58.0	57.5

its capability in reducing discrepancies and enhancing feature discrimination by features decorrelation.

VI. CONCLUSION

This paper presents a novel approach termed Density Ratio Regularization (*DEAR*) for the task of CC-ReID, which involves matching images of the same individual across different camera views or time points, accommodating variations in appearance due to factors like pose, lighting, and clothing changes. *DEAR* introduces an adversarial loss term designed to encourage the model to generate features that are decorrelated in each column.

To achieve this, we train a domain discriminator to differentiate between output features from the backbone network generated in its usual configuration and those produced from a batch-wise shuffle. The discriminator network then provides feedback to the backbone, guiding it to learn decorrelated features. Through extensive experiments on relevant datasets, our findings consistently demonstrate that *DEAR* surpasses the baseline method by a significant margin. The results highlight that the proposed adversarial loss effectively enhances the re-id model’s robustness against clothing changes and improves its overall generalization ability.

REFERENCES

- [1] W. Shi, H. Liu, and M. Liu, “Identity-sensitive loss guided and instance feature boosted deep embedding for person search,” *Neurocomputing*, vol. 415, pp. 1–14, 2020.
- [2] B. Ke, H. Zheng, L. Chen, Z. Yan, and Y. Li, “Multi-object tracking by joint detection and identification learning,” *Neural Processing Letters*, vol. 50, pp. 283–296, 2019.
- [3] X. Gu, H. Chang, B. Ma, H. Zhang, and X. Chen, “Appearance-preserving 3d convolution for video-based person re-identification,” in *Computer Vision—ECCV 2020: 16th European Conference, Glasgow, UK, August 23–28, 2020, Proceedings, Part II 16*. Springer, 2020, pp. 228–243.
- [4] K. Zhou, Y. Yang, A. Cavallaro, and T. Xiang, “Omni-scale feature learning for person re-identification,” in *Proceedings of the IEEE/CVF international conference on computer vision*, 2019, pp. 3702–3712.
- [5] L. Zheng, L. Shen, L. Tian, S. Wang, J. Wang, and Q. Tian, “Scalable person re-identification: A benchmark,” in *IEEE International Conference on Computer Vision*, 2015, pp. 1116–1124.
- [6] X. Gu, B. Ma, H. Chang, S. Shan, and X. Chen, “Temporal knowledge propagation for image-to-video person re-identification,” in *ICCV*, 2019.
- [7] R. Hou, B. Ma, H. Chang, X. Gu, S. Shan, and X. Chen, “Feature completion for occluded person re-identification,” *TPAMI*, 2021.
- [8] R. Geirhos, J.-H. Jacobsen, C. Michaelis, R. Zemel, W. Brendel, M. Bethge, and F. A. Wichmann, “Shortcut learning in deep neural networks,” *Nature Machine Intelligence*, vol. 2, no. 11, pp. 665–673, 2020.
- [9] M. Arjovsky, L. Bottou, I. Gulrajani, and D. Lopez-Paz, “Invariant risk minimization,” *arXiv preprint arXiv:1907.02893*, 2019.
- [10] Q. Yang, A. Wu, and W.-S. Zheng, “Person re-identification by contour sketch under moderate clothing change,” *IEEE transactions on pattern analysis and machine intelligence*, vol. 43, no. 6, pp. 2029–2046, 2019.
- [11] X. Qian, W. Wang, L. Zhang, F. Zhu, Y. Fu, T. Xiang, Y.-G. Jiang, and X. Xue, “Long-term cloth-changing person re-identification,” in *Proceedings of the Asian Conference on Computer Vision*, 2020.
- [12] F. Wan, Y. Wu, X. Qian, Y. Chen, and Y. Fu, “When person re-identification meets changing clothes,” in *Proceedings of the IEEE/CVF Conference on Computer Vision and Pattern Recognition Workshops*, 2020, pp. 830–831.
- [13] S. Yu, S. Li, D. Chen, R. Zhao, J. Yan, and Y. Qiao, “Cocas: A large-scale clothes changing person dataset for re-identification,” in *Proceedings of the IEEE Conference on Computer Vision and Pattern Recognition*, 2020, pp. 3400–3409.
- [14] J. Chen, X. Jiang, F. Wang, J. Zhang, F. Zheng, X. Sun, and W.-S. Zheng, “Learning 3d shape feature for texture-insensitive person re-identification,” in *Proceedings of the IEEE/CVF Conference on Computer Vision and Pattern Recognition*, 2021, pp. 8146–8155.
- [15] X. Gu, H. Chang, B. Ma, S. Bai, S. Shan, and X. Chen, “Clothes-changing person re-identification with rgb modality only,” in *Proceedings of the IEEE/CVF Conference on Computer Vision and Pattern Recognition*, 2022, pp. 1060–1069.
- [16] Z. Cui, J. Zhou, Y. Peng, S. Zhang, and Y. Wang, “Dcr-reid: Deep component reconstruction for cloth-changing person re-identification,” *IEEE Transactions on Circuits and Systems for Video Technology*, 2023.
- [17] Y. Sun, L. Zheng, Y. Yang, Q. Tian, and S. Wang, “Beyond part models: Person retrieval with refined part pooling (and a strong convolutional baseline),” in *Proceedings of the European conference on computer vision (ECCV)*, 2018, pp. 480–496.
- [18] K. He, X. Zhang, S. Ren, and J. Sun, “Deep residual learning for image recognition,” in *Proceedings of the IEEE conference on computer vision and pattern recognition*, 2016, pp. 770–778.
- [19] X. Qian, W. Wang, L. Zhang, F. Zhu, Y. Fu, T. Xiang, Y.-G. Jiang, and X. Xue, “Long-term cloth-changing person re-identification,” in *ACCV*, 2020.
- [20] Q. Yang, A. Wu, and W.-S. Zheng, “Person re-identification by contour sketch under moderate clothing change,” *TPAMI*, vol. 43, no. 6, pp. 2029–2046, 2021.
- [21] F. Wan, Y. Wu, X. Qian, and Y. Fu, “When person re-identification meets changing clothes,” in *CVPR Workshop*, 2020.
- [22] R. Shwartz-Ziv and N. Tishby, “Opening the black box of deep neural networks via information,” *arXiv preprint arXiv:1703.00810*, 2017.
- [23] A. Achille and S. Soatto, “Information dropout: Learning optimal representations through noisy computation,” *IEEE transactions on pattern analysis and machine intelligence*, vol. 40, no. 12, pp. 2897–2905, 2018.
- [24] N. Tishby and N. Zaslavsky, “Deep learning and the information bottleneck principle,” in *2015 IEEE information theory workshop (itw)*. IEEE, 2015, pp. 1–5.
- [25] X. Wang, G. Doretto, T. Sebastian, J. Rittscher, and P. Tu, “Shape and appearance context modeling,” in *ICCV*, 2007.
- [26] B. Ma, Y. Su, and F. Jurie, “Bicov: a novel image representation for person re-identification and face verification,” in *BMVC*, 2012.
- [27] E. Corvee, F. Bremond, M. Thonnat *et al.*, “Person re-identification using spatial covariance regions of human body parts,” in *AVSS*, 2010.
- [28] M. Farenzena, L. Bazzani, A. Perina, V. Murino, and M. Cristani, “Person re-identification by symmetry-driven accumulation of local features,” in *CVPR*, 2010.
- [29] M. Koestinger, M. Hirzer, P. Wohlhart, P. M. Roth, and H. Bischof, “Large scale metric learning from equivalence constraints,” in *CVPR*, 2012.
- [30] Z. Li, S. Chang, F. Liang, T. S. Huang, L. Cao, and J. R. Smith, “Learning locally-adaptive decision functions for person verification,” in *CVPR*, 2013.
- [31] D. Chen, Z. Yuan, B. Chen, and N. Zheng, “Similarity learning with spatial constraints for person re-identification,” in *CVPR*, 2016.
- [32] A. Mignon and F. Jurie, “Pcca: A new approach for distance learning from sparse pairwise constraints,” in *CVPR*, 2012.
- [33] W. Chen, X. Chen, J. Zhang, and K. Huang, “Beyond triplet loss: A deep quadruplet network for person re-identification,” in *CVPR*, 2017.
- [34] W. Li, X. Zhu, and S. Gong, “Harmonious attention network for person re-identification,” in *CVPR*, 2018.
- [35] D. Li, X. Chen, Z. Zhang, and K. Huang, “Learning deep context-aware features over body and latent parts for person re-identification,” in *CVPR*, 2017.
- [36] F. Wang, W. Zuo, L. Lin, D. Zhang, and L. Zhang, “Joint learning of single-image and cross-image representations for person re-identification,” in *CVPR*, 2016.
- [37] J. Xu, R. Zhao, F. Zhu, H. Wang, and W. Ouyang, “Attention-aware compositional network for person re-identification,” in *CVPR*, 2018.

- [38] T. Xiao, H. Li, W. Ouyang, and X. Wang, "Learning deep feature representations with domain guided dropout for person re-identification," in *CVPR*, 2016.
- [39] G. Wang, Y. Yuan, X. Chen, J. Li, and X. Zhou, "Learning discriminative features with multiple granularities for person re-identification," in *Proceedings of the 26th ACM international conference on Multimedia*, 2018, pp. 274–282.
- [40] Z. Gao, H. Zhang, L. Gao, Z. Cheng, and S. Chen, "Dcr: A unified framework for holistic/partial person reid," *IEEE Transactions on Multimedia*, vol. 23, pp. 3332–3345, 2021.
- [41] C. Song, Y. Huang, W. Ouyang, and L. Wang, "Mask-guided contrastive attention model for person re-identification," in *Proceedings of the IEEE Conference on Computer Vision and Pattern Recognition*, 2018, pp. 1179–1188.
- [42] J. Miao, Y. Wu, P. Liu, Y. Ding, and Y. Yang, "Pose-guided feature alignment for occluded person re-identification," in *Proceedings of the IEEE International Conference on Computer Vision*, 2019, pp. 542–551.
- [43] L. Gao, H. Zhang, Z. Gao, W. Guan, Z. Cheng, and M. Wang, "Texture semantically aligned with visibility-aware for partial person re-identification," in *MM '20: The 28th ACM International Conference on Multimedia, Virtual Event / Seattle, WA, USA, October 12-16, 2020*, pp. 3771–3779.
- [44] Q. Yang, A. Wu, and W.-S. Zheng, "Person re-identification by contour sketch under moderate clothing change," *IEEE Transactions on Pattern Analysis and Machine Intelligence*, vol. 43, no. 6, pp. 2029–2046, 2021.
- [45] Y. Huang, J. Xu, Q. Wu, Y. Zhong, P. Zhang, and Z. Zhang, "Beyond scalar neuron: Adopting vector-neuron capsules for long-term person re-identification," *IEEE Trans. Circuits Syst. Video Technol.*, vol. 30, no. 10, pp. 3459–3471, 2020.
- [46] K. Wang, Z. Ma, S. Chen, J. Yang, K. Zhou, and T. Li, "A benchmark for clothes variation in person re-identification," *International Journal of Intelligent Systems*, vol. 35, no. 12, pp. 1881–1898, 2020.
- [47] Z. Gao, H. Wei, W. Guan, W. Nie, M. Liu, and M. Wang, "Multigranular visual-semantic embedding for cloth-changing person re-identification," *CoRR*, vol. abs/2108.04527, 2021.
- [48] P. Hong, T. Wu, A. Wu, X. Han, and W. Zheng, "Fine-grained shape-appearance mutual learning for cloth-changing person re-identification," in *IEEE Conference on Computer Vision and Pattern Recognition, CVPR, virtual, June 19-25, 2021*, pp. 10 513–10 522.
- [49] X. Shu, G. Li, X. Wang, W. Ruan, and Q. Tian, "Semantic-guided pixel sampling for cloth-changing person re-identification," *IEEE Signal Processing Letters*, vol. 28, pp. 1365–1369, 2021.
- [50] Z. Yang, M. Lin, X. Zhong, Y. Wu, and Z. Wang, "Good is bad: Causality inspired cloth-debiasing for cloth-changing person re-identification," in *Proceedings of the IEEE/CVF Conference on Computer Vision and Pattern Recognition*, 2023, pp. 1472–1481.
- [51] Z. Yang, X. Zhong, Z. Zhong, H. Liu, Z. Wang, and S. Satoh, "Win-win by competition: Auxiliary-free cloth-changing person re-identification," *IEEE Transactions on Image Processing*, 2023.
- [52] P. P. Chan, X. Hu, H. Song, P. Peng, and K. Chen, "Learning disentangled features for person re-identification under clothes changing," *ACM Transactions on Multimedia Computing, Communications and Applications*, vol. 19, no. 6, pp. 1–21, 2023.
- [53] K. Han, S. Gong, Y. Huang, L. Wang, and T. Tan, "Clothing-change feature augmentation for person re-identification," in *Proceedings of the IEEE/CVF Conference on Computer Vision and Pattern Recognition*, 2023, pp. 22 066–22 075.
- [54] S. Lloyd, "Least squares quantization in pcm," *IEEE transactions on information theory*, vol. 28, no. 2, pp. 129–137, 1982.
- [55] M. Sugiyama, T. Suzuki, and T. Kanamori, *Density ratio estimation in machine learning*. Cambridge University Press, 2012.
- [56] T. Kanamori, T. Suzuki, and M. Sugiyama, "Statistical analysis of kernel-based least-squares density-ratio estimation," *Machine Learning*, vol. 86, pp. 335–367, 2012.
- [57] J. Qin, "Inferences for case-control and semiparametric two-sample density ratio models," *Biometrika*, vol. 85, no. 3, pp. 619–630, 1998.
- [58] K. F. Cheng and C.-K. Chu, "Semiparametric density estimation under a two-sample density ratio model," *Bernoulli*, vol. 10, no. 4, pp. 583–604, 2004.
- [59] Y. Tsuboi, H. Kashima, S. Hido, S. Bickel, and M. Sugiyama, "Direct density ratio estimation for large-scale covariate shift adaptation," *Journal of Information Processing*, vol. 17, pp. 138–155, 2009.
- [60] Y. Huang, J. Xu, Q. Wu, Y. Zhong, P. Zhang, and Z. Zhang, "Beyond scalar neuron: Adopting vector-neuron capsules for long-term person re-identification," *TCSVT*, vol. 30, no. 10, pp. 3459–3471, 2020.
- [61] P. Hong, T. Wu, A. Wu, X. Han, and W.-S. Zheng, "Fine-grained shape-appearance mutual learning for cloth-changing person re-identification," in *CVPR*, 2021.
- [62] J. Chen, X. Jiang, F. Wang, J. Zhang, F. Zheng, X. Sun, and W.-S. Zheng, "Learning 3d shape feature for texture-insensitive person re-identification," in *CVPR*, 2021.
- [63] Y.-J. Li, X. Weng, and K. M. Kitani, "Learning shape representations for person re-identification under clothing change," in *Proceedings of the IEEE/CVF Winter Conference on Applications of Computer Vision*, 2021, pp. 2432–2441.
- [64] H. Luo, Y. Gu, X. Liao, S. Lai, and W. Jiang, "Bag of tricks and a strong baseline for deep person re-identification," in *Proceedings of the IEEE/CVF conference on computer vision and pattern recognition workshops*, 2019, pp. 0–0.
- [65] Y. Suh, J. Wang, S. Tang, T. Mei, and K. M. Lee, "Part-aligned bilinear representations for person re-identification," in *ECCV*, 2018.
- [66] X. Fan, H. Luo, X. Zhang, L. He, C. Zhang, and W. Jiang, "Scpnet: Spatial-channel parallelism network for joint holistic and partial person re-identification," in *Computer Vision—ACCV 2018: 14th Asian Conference on Computer Vision, Perth, Australia, December 2–6, 2018, Revised Selected Papers, Part II 14*. Springer, 2019, pp. 19–34.
- [67] C. Eom and B. Ham, "Learning disentangled representation for robust person re-identification," *Advances in neural information processing systems*, vol. 32, 2019.
- [68] Z. Zheng, X. Yang, Z. Yu, L. Zheng, Y. Yang, and J. Kautz, "Joint discriminative and generative learning for person re-identification," in *proceedings of the IEEE/CVF conference on computer vision and pattern recognition*, 2019, pp. 2138–2147.
- [69] S. He, H. Luo, P. Wang, F. Wang, H. Li, and W. Jiang, "Transreid: Transformer-based object re-identification," in *Proceedings of the IEEE/CVF International Conference on Computer Vision (ICCV)*, October 2021, pp. 15 013–15 022.
- [70] X. Qian, Y. Fu, Y.-G. Jiang, T. Xiang, and X. Xue, "Multi-scale deep learning architectures for person re-identification," in *ICCV*, 2017.
- [71] Y. Huang, Q. Wu, J. Xu, Y. Zhong, and Z. Zhang, "Clothing status awareness for long-term person re-identification," in *ICCV*, 2021.
- [72] S. Ioffe and C. Szegedy, "Batch normalization: Accelerating deep network training by reducing internal covariate shift," in *ICML*, 2015.
- [73] Z. Zhong, L. Zheng, G. Kang, S. Li, and Y. Yang, "Random erasing data augmentation," in *AAAI*, 2020.
- [74] D. P. Kingma and J. Ba, "Adam: A method for stochastic optimization," in *ICLR*, 2015.
- [75] B. Zhou, A. Khosla, A. Lapedriza, A. Oliva, and A. Torralba, "Learning deep features for discriminative localization," in *Proceedings of the IEEE conference on computer vision and pattern recognition*, 2016, pp. 2921–2929.
- [76] K. Zhou, Y. Yang, A. Cavallaro, and T. Xiang, "Omni-scale feature learning for person re-identification," in *ICCV*, 2019.
- [77] H. Luo, Y. Gu, X. Liao, S. Lai, and W. Jiang, "Bag of tricks and a strong baseline for deep person re-identification," in *CVPR Workshops*, 2019.
- [78] X. Shu, X. Wang, S. Zhang, X. Zhang, Y. Chen, G. Li, and Q. Tian, "Large-scale spatio-temporal person re-identification: Algorithm and benchmark," *arXiv preprint arXiv: 2105.15076*, 2021.
- [79] P. Xu and X. Zhu, "Deepchange: A large long-term person re-identification benchmark with clothes change," *arXiv preprint arXiv:2105.14685*, 2021.
- [80] L. Van der Maaten and G. Hinton, "Visualizing data using t-sne." *Journal of machine learning research*, vol. 9, no. 11, 2008.



Hongjun Wang is a Ph.D. candidate in Mechano-Informatics at The University of Tokyo. He holds an M.S. degree in Computer Science and Technology from Southern University of Science and Technology, China, and a B.E. degree from Nanjing University of Posts and Telecommunications, China. His research spans multiple areas, including machine learning, computer vision, urban computing, data mining, and data visualization.



Jiyuan Chen is a Ph.D. candidate in Department of Computing, The Hong Kong Polytechnic University. He holds a B.E. degree from Southern University of Science and Technology, China. His research interests are diverse, including fields such as machine learning, image restoration, urban computing.



Renhe Jiang received a B.S. degree in software engineering from the Dalian University of Technology, China, in 2012, a M.S. degree in information science from Nagoya University, Japan, in 2015, and a Ph.D. degree in civil engineering from The University of Tokyo, Japan, in 2019. From 2019, he has been an Assistant Professor at the Information Technology Center, The University of Tokyo. His research interests include ubiquitous computing, deep learning, and spatio-temporal data analysis.



Prof. Xuan Song received the Ph.D. degree in signal and information processing from Peking University in 2010. In 2017, he was selected as Excellent Young Researcher of Japan MEXT. He served as Associate Editor, Guest Editor, Area Chair, Senior Program Committee Member for many famous journals and top-tier conferences, such as IMWUT, IEEE Transactions on Multimedia, WWW Journal, ACM TIST, IEEE TKDE, Big Data Journal, UbiComp, IJCAI, AAAI, ICCV, CVPR and etc. His main research interest are AI and its related research areas, such

as data mining and urban computing. By now, he has published more than 160 technical publications in journals, book chapter, and international conference proceedings, including more than 110 high-impact papers in top-tier publications for computer science. His research was featured in many Chinese, Japanese and international media, including United Nations, the Discovery Channel, and Fast Company Magazine. He received Honorable Mention Award in UbiComp 2015.



Prof. Yinqiang Zheng (Senior Member, IEEE) received the bachelor's degree from the Department of Automation, Tianjin University, Tianjin, China, in 2006, the Master of Engineering degree from Shanghai Jiao Tong University, Shanghai, China, in 2009, and the Doctoral of Engineering degree from the Department of Mechanical and Control Engineering, Tokyo Institute of Technology, Tokyo, Japan, in 2013. He is currently an associate professor with the University of Tokyo, Tokyo. He was program committee member for major international conferences,

like CVPR, ICCV, ECCV, ICLR, NeurIPS, AAAI, IJCAI, MICCAI, area chair for MVA2017, DICTA2018, ISAIR2019, ACCV2020, 3DV2020, ICCV2021, workshop co-organizer for ICPR2018 and ICCV2019, guest editor for Pattern Recognition Letter and Sensors. He is a Member of ACM.